The EMBO Journal (2012) 31, 1692–1703 | © 2012 European Molecular Biology Organization | All Rights Reserved 0261-4189/12
www.embojournal.org

THE EMBO JOURNAL

Axl is essential for VEGF-A-dependent activation of PI3K/Akt

Guo-Xiang Ruan and Andrius Kazlauskas*

Schepens Eye Research Institute, Massachusetts Eye and Ear Infirmary, Department of Ophthalmology, Harvard Medical School, Boston, MA, USA

Herein, we report that vascular endothelial growth factor A (VEGF-A) engages the PI3K/Akt pathway by a previously unknown mechanism that involves three tyrosine kinases. Upon VEGF-A-dependent activation of VEGF receptor-2 (VEGFR-2), and subsequent TSAd-mediated activation of Src family kinases (SFKs), SFKs engage the receptor tyrosine kinase Axl via its juxtamembrane domain to trigger ligand-independent autophosphorylation at a pair of YXXM motifs that promotes association with PI3K and activation of Akt. Other VEGF-A-mediated signalling pathways are independent of Axl. Interfering with Axl expression or function impairs VEGF-A- but not bFGF-dependent migration of endothelial cells. Similarly, Axl null mice respond poorly to VEGF-A-induced vascular permeability or angiogenesis, whereas other agonists induce a normal response. These results elucidate the mechanism by which VEGF-A activates PI3K/Akt, and identify previously unappreciated potential therapeutic targets of VEGF-A-driven processes.

The EMBO Journal (2012) **31,** 1692–1703. doi:10.1038/emboj.2012.21; Published online 10 February 2012
Subject Categories: signal transduction; molecular biology of disease
Keywords: angiogenesis; Axl; PI3K; VEGF-A; VEGFR-2

Introduction

Vascular endothelial growth factor A (VEGF-A) is critical for vascular development and angiogenesis, that is, formation of new blood vessels from existing capillaries (Cross *et al*, 2003; Olsson *et al*, 2006). Loss of a single *vegfa* allele leads to abnormal blood vessel development and embryonic lethality at embryonic day 11–12 (Carmeliet *et al*, 1996; Ferrara *et al*, 1996). As a pro-angiogenic factor, VEGF-A stimulates survival, proliferation and migration of endothelial cells, and promotes vascular permeability (Pandya *et al*, 2006). Due to its essential role in angiogenesis, VEGF-A has received great attention as a target for therapeutics in the past decade. The FDA approved bevacizumab (Avastin), a humanized monoclonal anti-VEGF-A antibody, for the first-line treatment of patients with several cancers, in combination with conventional chemotherapy (Kerbel, 2008; Ferrara, 2009). In addition, intravitreal anti-VEGF-A therapy has emerged as a new approach to treat neovascular eye diseases. Ranibizumab (Lucentis), an antibody fragment developed from bevacizumab, is an FDA-approved treatment for neovascular age-related macular degeneration (AMD) (Brown *et al*, 2006; Rosenfeld *et al*, 2006). A disadvantage of anti-VEGF-A therapy is that it may inference with the physiological functions of VEGF-A. For example, in animal models of ischaemia-induced neovascularization, anti-VEGF-A therapy resulted in a significant loss of retinal ganglion cells (Nishijima *et al*, 2007). In this regard, approaches that prevent VEGF-A-dependent neovascular pathology without affecting the physiological functions of VEGF-A would be a welcome addition to current anti-VEGF-A therapy.

Many pro-angiogenic effects of VEGF-A are mediated by VEGF receptor 2 (VEGFR-2, also known as KDR or Flk-1) (Ferrara *et al*, 2003; Holmes *et al*, 2007). Binding of VEGF-A to VEGFR-2 activates the receptor's kinase activity and engages signalling enzymes such as Type Ia phosphoinositide 3-kinase (PI3K) and its downstream effector Akt, which are essential for cellular responses intrinsic to angiogenesis such as survival, migration and tube formation (Matsumoto and Claesson-Welsh, 2001; Im and Kazlauskas, 2006; Rahimi, 2006). Forced expression of a constitutively active mutant of Akt in endothelial cells leads to formation of hyperpermeable blood vessels in multiple non-tumour tissues, which recapitulates the structural and functional abnormalities of tumour blood vessels (Phung *et al*, 2006). While these studies identify PI3K/Akt as viable therapeutic candidates, using existing pharmacological inhibitors to block neovascularization would probably cause a plethora of intolerable adverse side effects due to the fact that the PI3K/Akt pathway is intrinsic to many physiological functions. A more plausible way to inhibit VEGF-A-driven neovascularization would be to selectively block VEGF-A/VEGFR-2-dependent PI3K/Akt activation. The roadblock to implementing such a strategy is our incomplete understanding of the mechanism by which VEGFR-2 activates PI3K/Akt.

Axl is a member of the TAM family of receptor tyrosine kinases (RTKs), which also includes Tyro3 and Mer. Studies with mice lacking multiple members of this family demonstrate a key role in regulating innate immunity (Rothlin *et al*, 2007). The ligand for all three TAM family members is Gas6 (Varnum *et al*, 1995). Axl is also implicated in metastasis of tumours, which often overexpress Axl (Holland *et al*, 2010). Axl is expressed in many cell types but is most prominent in the vasculature (Melaragno *et al*, 1999). While it is known that silencing Axl impaired angiogenesis, tube formation and cellular responses intrinsic to angiogenesis (Holland *et al*, 2005; Li *et al*, 2009), how Axl contributes to these events has not been investigated. Furthermore, there are no publications implicating a role for Axl in VEGF-A-mediated activation of the PI3K/Akt pathway.

RTKs typically activate Type Ia PI3K by inducing tyrosine phosphorylation of a Tyr-Xaa-Xaa-Met (YXXM) motif, which creates a docking site for SH2 domains of the p85 regulatory

*Corresponding author. Schepens Eye Research Institute, Massachusetts Eye and Ear Infirmary, Department of Ophthalmology, Harvard Medical School, 20 Staniford Street, Boston, MA 02114, USA. Tel.: +1 617 912 2517; Fax: +1 617 912 0101; E-mail: ak@eri.harvard.edu

Received: 4 November 2011; accepted: 16 January 2012; published online: 10 February 2012

subunit of PI3K (Cully *et al*, 2006). This process is currently known to proceed either by autophosphorylation at tyrosine residues within a YXXM motif (e.g., PDGFRs; Kazlauskas and Cooper, 1989), or by receptor-mediated phosphorylation of YXXM motif-containing adaptor proteins (e.g., insulin receptor substrates; Whitehead *et al*, 2000). Since VEGF-A does not trigger autophosphorylation of VEGFR-2 within a YXXM motif, it is likely that VEGFR-2 promotes tyrosine phosphorylation of a YXXM motif-containing adaptor protein. Our efforts to identify such a protein revealed a novel mechanism by which RTKs engage the PI3K/Akt pathway. VEGFR-2, acting through Src family kinases (SFKs), activates Axl in a ligand-independent manner leading to its autophosphorylation at YXXM tyrosines and consequent activation of the PI3K/Akt pathway.

Results

Identification of a candidate adaptor protein for VEGF-A-dependent activation of PI3K/Akt

Grb2-adaptor binder 1 (Gab1) has been implicated in mediating VEGF-A-dependent activation of PI3K/Akt at early time points post VEGF-A stimulation (Dance *et al*, 2006; Laramee *et al*, 2007). Surprisingly, when we silenced Gab1 expression in porcine aortic endothelial (PAE) cells stably expressing human VEGFR-2 (PAE/KDR cells) using two different Gab1 shRNAs, activation of Akt was not significantly changed at 5, 20 or 60 min post VEGF-A stimulation (Supplementary Figure S1). We thus speculated that in PAE/KDR cells, YXXM motif-containing proteins other than Gab1 are inducibly tyrosine phosphorylated by VEGF-A to activate PI3K/Akt. Note that VEGF-A-dependent activation of Akt in PAE/KDR cells was completely blocked by the PI3K inhibitor LY294002 (unpublished observations), indicating that Akt is a good indicator of PI3K activation in response to VEGF-A stimulation. In addition, VEGF-A did not induce activation of Akt in parental PAE, which do not express a detectable level of VEGFR-2 (unpublished observations), indicating that VEGFR-2 receptor is required for VEGF-A-induced activation of PI3K/Akt in PAE/KDR cells.

To identify proteins that are inducibly tyrosine phosphorylated by VEGF-A and associate with the p85 regulatory subunit of PI3K, we performed a Glutathione-S-Transferase (GST) pull-down assay with lysates of PAE/KDR cells using a fusion protein of GST and the N-terminal SH2 domain of human p85α (GST-p85SH2). The pull-down assay recovered three species (250, 140, 70 kDa) that were inducibly tyrosine phosphorylated by VEGF-A and associated with the SH2 domain of p85 (Figure 1A). The size of Gab1 is 110 kDa, and therefore it was unlikely to be one of the three species. The most prominent of the three was the 140-kDa species and its intensity was temporally correlated with Akt activation (Figure 1B). Moreover, the 140-kDa species was the only one that was tyrosine phosphorylated by VEGF-A and recovered with the p85 SH2 domain in human umbilical vein endothelial cells (HUVECs) (Supplementary Figure S2). Collectively, these data identified the 140-kDa species as a candidate adaptor protein that couples activated VEGFR-2 to PI3K activation.

Axl is required for VEGF-A-dependent activation of PI3K/Akt

The *SH2 domain* (http://sh2.uchicago.edu/) site lists 125 proteins that interact with the p85α subunit of PI3K, and 51 of them have a YXXM motif (http://scansite.mit.edu/). Fifteen of these YXXM motif-containing proteins are expressed in endothelial cells and have molecular mass of 120–150 kDa. One member of this list is the RTK Axl, which harbours two YXXM motifs that are needed for Axl to associate with the p85 subunit of PI3K (Braunger *et al*, 1997). Axl has been implicated in angiogenesis because of its ability to promote angiogenically related cellular responses in endothelial cells (Holland *et al*, 2005). Furthermore, an Axl kinase inhibitor suppresses angiogenesis driven by a VEGF-A-laden pellet implanted in the corneas of mice (Holland *et al*, 2010). While these reports support the idea that Axl is in some way pro-angiogenic, one group reported that the Axl ligand Gas6 antagonized VEGF-A-dependent signalling and cellular responses (Gallicchio *et al*, 2005). No publications address if Axl contributes to VEGF-A-dependent activation of PI3K/Akt.

We initiated a series of experiments to investigate the role of Axl in VEGF-A-dependent activation of PI3K/Akt. In PAE/KDR cells, HUVECs and human retinal microvascular endothelial cells (HRMECs) VEGF-A promoted Axl tyrosine phosphorylation and its association with p85 in a manner that temporally correlated with Akt activation (Figure 1C and D; Supplementary Figure S3). Furthermore, in Axl knockdown PAE/KDR cells or HUVECs, VEGF-A-dependent activation of Akt was suppressed (Figure 2A; Supplementary Figure S4). A pharmacological approach, using the Axl kinase inhibitor R428 (Holland *et al*, 2010), indicated that the Axl kinase activity was required for VEGF-A-dependent activation of Akt in HUVECs (Figure 2B). Furthermore, a dominant-negative mutant of Axl (consisting of the extracellular, transmembrane and juxtamembrane (JM) domains) suppressed Akt activation in response to VEGF-A in PAE/KDR cells (Supplementary Figure S5). Re-expressing wild type (Axlwt) in Axl knockdown PAE/KDR cells rescued VEGF-A-dependent activation of Akt (Supplementary Figure S6), supporting the idea that Axl was the relevant target of the Axl shRNA. We also isolated mouse heart endothelial cells (MHECs) from wild-type and Axl knockout (KO) mice. In Axl KO mice, exons 1–11 of *axl* are replaced by a bacterial *lacZ* gene. Axl KO mice are viable and fertile (Lu *et al*, 1999); and as expected, no Axl protein was detected in MHECs or the lung lysates prepared from Axl KO mice (Figure 2C; Supplementary Figure S7). VEGF-A-dependent activation of Akt was greatly attenuated in MHECs isolated from Axl KO mice (Figure 2C). Thus, four different approaches indicate that Axl is required for VEGF-A-dependent activation of Akt.

To test the importance of the tyrosines in the YXXM motif for VEGF-A-dependent activation of PI3K/Akt, we re-expressed the F73/15 mutant (Y773 and Y815 mutated to phenylalanine) in Axl knockdown cells. In contrast to the WT Axl, this mutant failed to rescue activation of Akt in response to VEGF-A stimulation (Supplementary Figure S6). These studies support the idea that Axl is the YXXM motif-containing protein that promotes VEGF-A-dependent activation of PI3K/Akt.

Unlike the reliance of Akt activation on Axl, VEGF-A-dependent engagement of other signalling enzymes was unaffected by any of the approaches that interfere with Axl expression or function (Figure 2; Supplementary Figure S4). For instance, the Axl kinase inhibitor R428 did not prevent VEGF-A-triggered activation of Src in HUVECs (Figure 2B).

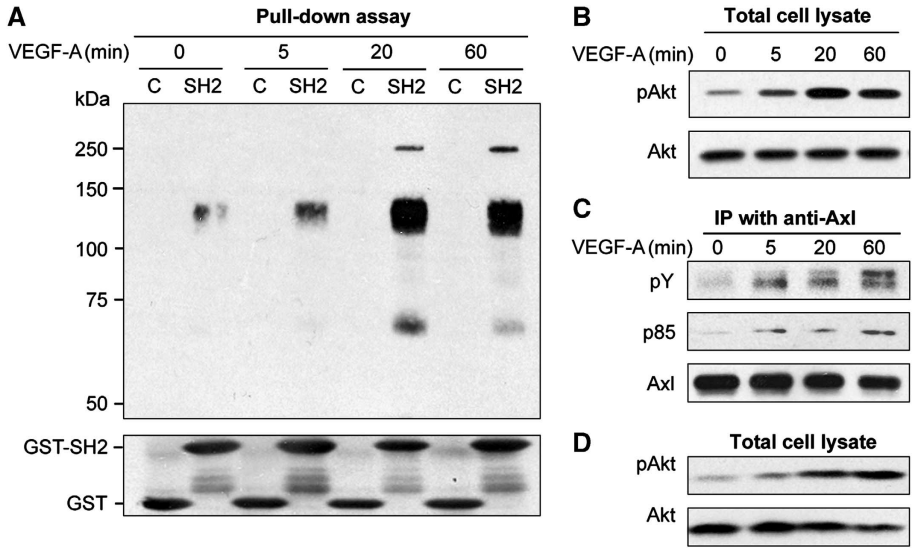

Figure 1 Identification of a candidate adaptor protein for VEGF-A-dependent activation of PI3K/Akt. (**A**) Three VEGF-A-dependent species are recovered in a GST-p85SH2 pull-down assay. Serum-starved PAE/KDR cells were pretreated with 100 μM sodium orthovanadate (an inhibitor of protein tyrosine phosphatases) for 1 h, then either left resting, or stimulated with 2.5 ng/ml VEGF-A for 5, 20 or 60 min. The clarified lysates were incubated with glutathione-agarose beads containing GST alone (C) or GST-p85SH2 fusion protein (SH2). The proteins bound to the GST or GST-p85SH2 fusion protein were resolved by SDS–PAGE and analysed by western blot analysis with an anti-phosphotyrosine (1:1 of PY20 and 4G10) antibody. The molecular weights of the three VEGF-A-dependent phosphoprotein bands that were recovered with the GST-p85SH2 fusion protein were ~250, 140 and 70 kDa. The membrane was stripped and reprobed with a GST antibody to assess the amount of fusion protein in each sample (bottom panel). (**B**) Total cell lysates used for the pull-down assay were blotted with pAkt (S473) antibody; the membrane was subsequently stripped and reprobed with a pan-Akt antibody. (**C**) VEGF-A promotes tyrosine phosphorylation of Axl and its association with p85. Serum-starved PAE/KDR cells were pretreated with sodium orthovanadate (100 μM) for 1 h, then stimulated with 2.5 ng/ml VEGF-A for the indicated times. The clarified lysates were immunoprecipitated with an anti-Axl antibody. The resulting samples were subjected to western blot analysis using the indicated antibodies. pY, 1:1 of PY20 and 4G10. (**D**) Total cell lysates used for immunoprecipitation were blotted with pAkt (S473) antibody, and the membrane was stripped and reprobed with a pan-Akt antibody. Figure source data can be found in Supplementary data.

Furthermore, other pro-angiogenic growth factors that activated Akt did so in an Axl-independent manner; bFGF promoted comparable activation of Akt in control and Axl knockdown PAE/KDR cells, and in MHEC cells from WT and Axl KO mice (Figure 2A and C).

Taken together, the data demonstrate that Axl mediates activation of PI3K/Akt, but not Erk or Src in VEGF-A-stimulated cells. In addition, the reliance on Axl maybe unique to VEGF-A, as it is not shared with other pro-angiogenic growth factors.

Axl does not appear to modulate VEGFR-2

In light of the findings described above, we further investigated the relationship between VEGFR-2 and Axl. In contrast to the ability of VEGF-A to increase tyrosine phosphorylation of Axl (Figure 1C; Supplementary Figures S3 and S8), activation of Axl with its ligand Gas6 did not promote tyrosine phosphorylation of VEGFR-2 (Supplementary Figure S8). Furthermore, Gas6-mediated tyrosine phosphorylation of Axl was comparable in cells that do and do not express VEGFR-2 (Supplementary Figure S9). These data indicate that while VEGF-A promotes tyrosine phosphorylation of Axl, the reciprocal relationship does not appear to exist. In addition, Gas6-mediated activation of Axl proceeds independently of VEGFR-2.

An additional facet of the Axl/VEGFR-2 relationship that we considered was the previously reported ability of Gas6 to inhibit VEGF-A-dependent activation of VEGFR-2 (Gallicchio *et al*, 2005). We did not find this to be the case. VEGFR-2 tyrosine phosphorylation and activation of Akt and Erk were comparable in HUVECs stimulated with VEGF-A alone or with the combination of VEGF-A and Gas6 (Supplementary Figure S8). Furthermore, the combined stimulation resulted in greater activation of certain signalling events (e.g., Src) as compared with the response achieved when only one agent was added (Supplementary Figure S8).

SFKs and Axl collaborate to activate PI3K/Akt in response to VEGF-A

We considered the mechanism by which VEGFR-2 engages Axl/Akt. One possibility is that activated VEGFR-2 promotes secretion of Gas6, which activates Axl and hence PI3K/Akt. However, this does not appear to be the case. While a Gas6 trap (AxlFc) effectively blocked Gas6-induced activation of Akt, it did not interfere with this event in VEGF-A-stimulated cells (Supplementary Figure S10). In light of these findings, and the absence of publications indicating a pro-angiogenic role for Gas6, we abandoned the possibility that Gas6 contributes to VEGF-A-dependent activation of Axl/Akt.

Instead of an extracellular mechanism, we wondered if VEGFR-2 engaged Axl/Akt intracellularly. We focused on SFKs because they are activated by VEGF-A (Olsson *et al*, 2006; Figures 2B and 3A) and Gas6-mediated activation of Axl requires SFKs (Supplementary Figure S11). To focus on the pool of SFKs that are activated by VEGF-A/VEGFR-2, we generated HUVECs with reduced expression of T cell-specific adaptor protein (TSAd; also called VRAP or SH2D2A), which is required for VEGF-A-dependent activation of SFKs (Matsumoto *et al*, 2005). In TSAd knockdown HUVECs, VEGF-A-dependent activation of Axl/Akt was reduced

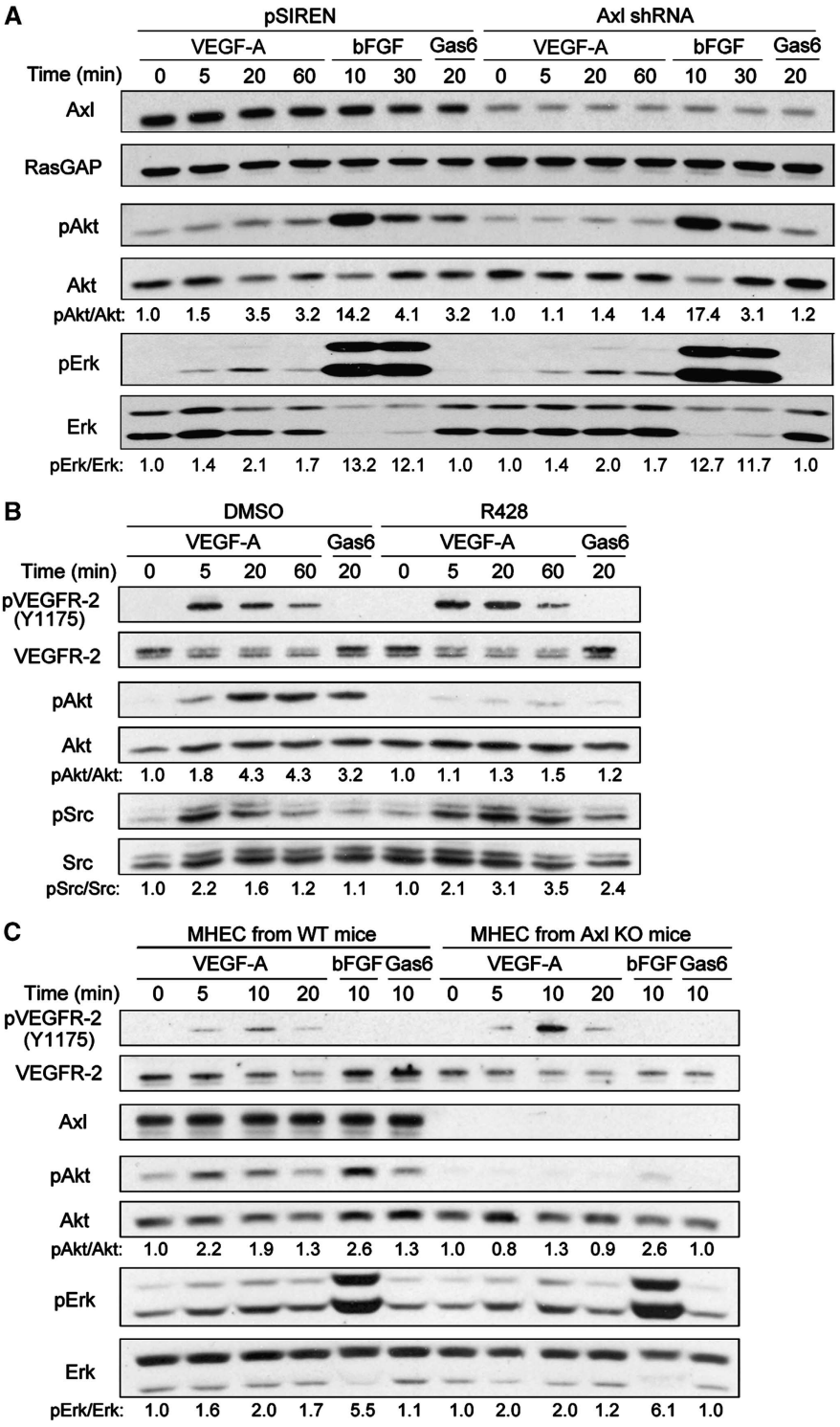

Figure 2 Axl is required for VEGF-A-dependent activation of PI3K/Akt. (**A**) Silencing Axl expression attenuates VEGF-A-dependent activation of Akt. Serum-starved PAE/KDR cells stably expressing either an empty vector (pSIREN) or Axl shRNA were treated with VEGF-A (2.5 ng/ml), bFGF (10 ng/ml), or the endogenous Axl ligand Gas6 (100 ng/ml) for the indicated times. Cell lysates were subjected to western blot analysis using the indicated antibodies. Axl shRNA reduced Axl level by ~86% (Axl levels were normalized to RasGAP levels). The ratios of pAkt/Akt and pErk/Erk are shown at the bottom; the pAkt/Akt or pErk/Erk ratio for unstimulated cells is normalized to 1.0. Silencing Axl reduced Gas6- and VEGF-A-induced Akt activation, but not bFGF-induced Akt activation. In addition, the kinetics and amplitude of Erk activation were not markedly influenced by suppressing expression of Axl. (**B**) VEGF-A-dependent activation of PI3K/Akt is suppressed by the Axl inhibitor R428. Serum-starved HUVECs were pretreated with the Axl inhibitor R428 (50 nM) or DMSO for 30 min, then treated with VEGF-A (2.5 ng/ml) or Gas6 (100 ng/ml) for the indicated times. Cell lysates were subjected to western blot analysis using the indicated antibodies. R428 markedly inhibited both Gas6- and VEGF-A-induced activation of Akt, but not VEGF-A-induced activation of VEGFR-2 and Src. (**C**) VEGF-A-dependent activation of Akt is attenuated in MHECs prepared from Axl null mice. Serum-starved MHECs cells were treated with VEGF-A (10 ng/ml), bFGF (10 ng/ml) or Gas6 (100 ng/ml) for the indicated times. Cell lysates were subjected to western blot analysis using the indicated antibodies. Axl was not detected in MHECs prepared from Axl KO mice. Eliminating Axl in MHECs attenuated VEGF-A-induced activation of Akt, but not activation of VEGFR-2 and Erk. Responses to bFGF remained intact in Axl null MHECs. Figure source data can be found in Supplementary data.

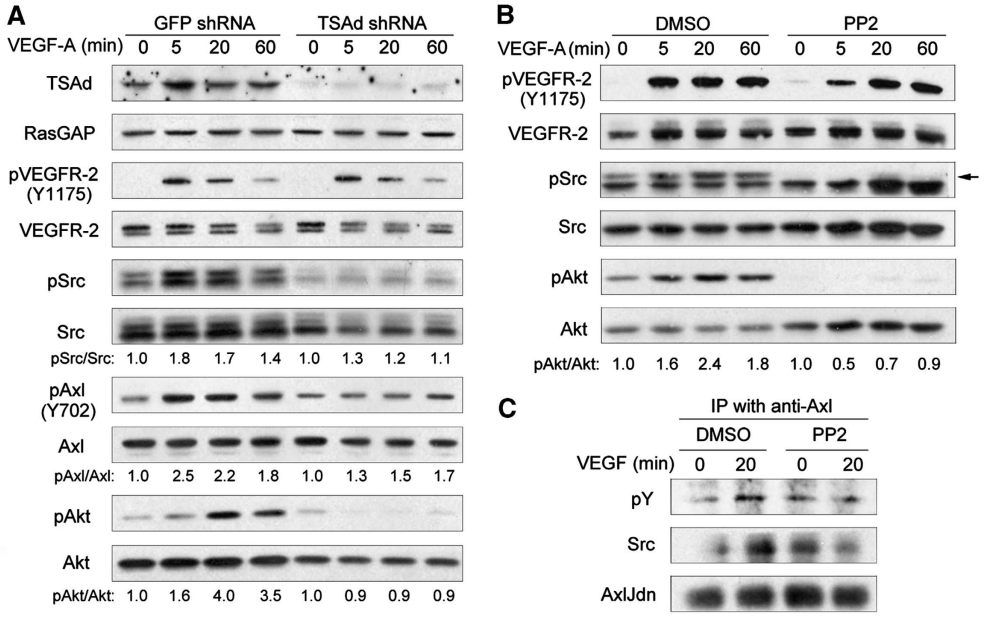

Figure 3 SFKs are essential to VEGF-A-dependent activation of PI3K/Akt. (**A**) TSAd signals upstream of SFKs, Axl and PI3K/Akt in response to VEGF-A. Serum-starved HUVECs stably expressing GFP shRNA or TSAd shRNA were treated with VEGF-A (2.5 ng/ml) for the indicated times. Cell lysates were subjected to western blot analysis using the indicated antibodies. TSAd shRNA reduced TSAd level by ~80% (TSAd levels were normalized to RasGAP levels). Silencing TSAd markedly decreased VEGF-A-driven activation of Src, Axl and Akt. (**B**) VEGF-A-dependent activation of PI3K/Akt is dependent on SFKs. Serum-starved PAE/KDR cells were pretreated with the SFK inhibitor PP2 (10 μM) or DMSO for 30 min, then treated with VEGF-A for the indicated times. Total cell lysates were subjected to western blot analysis using the indicated antibodies. The upper band in the pSrc blot (arrow) is the specific pSrc band in PAE/KDR cells. (**C**) VEGF-A promotes tyrosine phosphorylation of the JM domain of Axl and its association with Src. Serum-starved PAE/KDR cells expressing AxlJdn (includes the extracellular, transmembrane and JM domains of mouse Axl) were pretreated with sodium orthovanadate (100 μM) for 1 h, and pretreated with the SFK inhibitor PP2 (10 μM) or DMSO for 30 min, then either left resting, or treated with 2.5 ng/ml VEGF-A for 20 min. The clarified lysates were immunoprecipitated with an anti-Axl antibody that recognizes the extracellular domain of mouse Axl. This antibody does not recognize endogenous, porcine Axl. The resulting samples were subjected to western blot analysis using the indicated antibodies. pY, 1:1 of PY20 and 4G10. VEGF-A stimulated AxlJdn tyrosine phosphorylation and its association with Src, which were suppressed by the SFK inhibitor PP2. Figure source data can be found in Supplementary data.

(Figure 3A). Furthermore, globally inhibiting SFKs with either PP2 (Figure 3B) or SU6656 (unpublished observations) also blocked VEGF-A-induced activation of Akt. To determine if activation of SFKs was sufficient to activate PI3K/Akt, we made use of a mutant version of Src (R388A) whose kinase activity is rescued upon binding the small molecule imidazole (Qiao *et al*, 2006; Im and Kazlauskas, 2007). Imidazole increased Src activity and phosphorylation of Akt in R388A-expressing cells, but not in control cells, which expressed D386N Src mutant that is unresponsive to imidazole (Figure 4A), indicating that activating Src is sufficient to activate PI3K/Akt. Furthermore, the pathway by which Src activated PI3K/Akt was at least in part dependent on Axl, since reducing expression of Axl in R388A cells attenuated imidazole-dependent phosphorylation of Akt (Figure 4B). Taken together, these studies support the idea that VEGFR-2 engages Axl/Akt intracellularly, and that SFKs are an essential member of this pathway.

In light of the fact that the Axl JM domain contains tyrosines within an SFK consensus phosphorylation site (http://scansite.mit.edu/), we tested the possibility that SFKs phosphorylated Axl in the JM domain. Indeed, VEGF-A promoted tyrosine phosphorylation of dominant-negative Axl in which the JM domain constitutes the entire intracellular portion, and this event was blocked by the SFK kinase inhibitor PP2 (Figure 3C). The SH2 domain of SFKs prefers phosphotyrosines in a context corresponding to the SFK consensus phosphorylation site (Songyang *et al*, 1995). Consequently, it was likely that SFKs would also bind to Axl after phosphorylating it, similarly to what is observed in the relationship between SFKs and PDGFRs (Kypta *et al*, 1990). Indeed, in accordance with the VEGF-A-mediated increase in tyrosine phosphorylation of the JM domain of Axl, there was an increase in the amount of co-precipitating Src (Figure 3C). These studies indicated that VEGF-A promoted both SFK-dependent phosphorylation of, and association with the JM domain of Axl.

Additional evidence for an involvement of the JM domain of Axl and the tyrosine residues in particular emerged from the observations that the efficiency of the dominant-negative Axl mutant declined substantially when the JM domain was eliminated (Supplementary Figure S5) or the three tyrosine residues in the Axl JM domain were mutated to phenylalanines (Supplementary Figure S12).

It is known that SFKs can phosphorylate the JM domain of RTKs and thereby relieve the autoinhibition that it exerts on its kinase activity (Wybenga-Groot *et al*, 2001; Rohde *et al*, 2004). If SFKs were performing a similar function on Axl in VEGF-A-stimulated cells, then kinase inactive Axl would be unable to autophosphorylate and thereby engage the PI3K/Akt pathway. Indeed, while re-expression of WT Axl in Axl knockdown cells rescued VEGF-A-mediated activation of Akt, kinase inactive Axl (AxlK561R) (McCloskey *et al*, 1997) did not (Supplementary Figure S13).

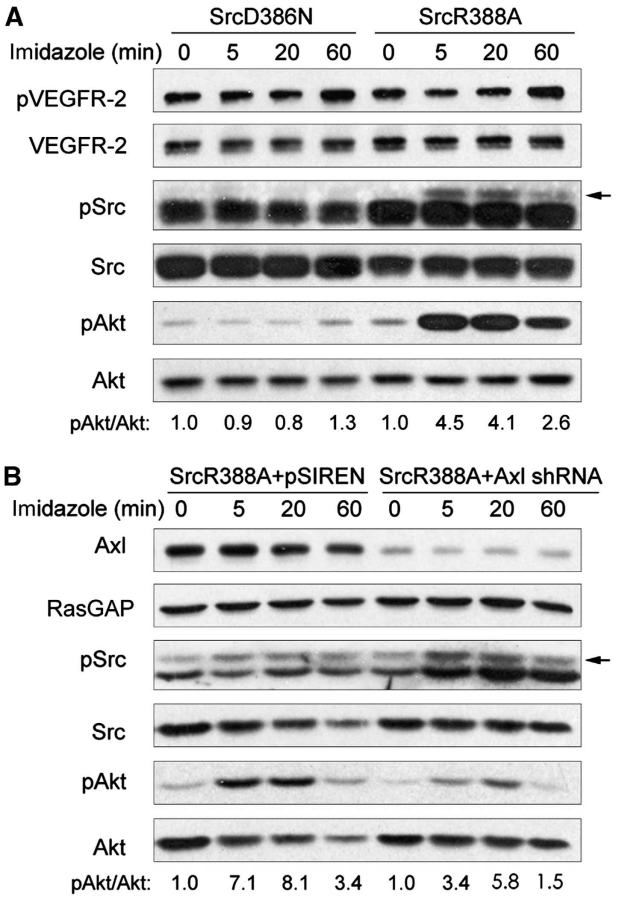

Figure 4 Selectively activating Src is sufficient to activate PI3K/Akt, which is partially dependent on Axl. (**A**) Selectively activating Src is sufficient to activate Akt. Serum-starved PAE/KDR cells expressing R388A or D386N mutants were treated with imidazole (5 mM) for the indicated times. Total cell lysates were subjected to western blot analysis using the indicated antibodies. Imidazole induced activation of Src (arrow) and Akt in the R388A mutant but not in the D386N mutant. (**B**) Src-induced activation of Akt is partially dependent on Axl. PAE/KDR cells expressing Src R388A were infected with a retrovirus harbouring Axl shRNA or the empty vector pSIREN. Serum-starved cells were treated with imidazole (5 mM) for the indicated times. Total cell lysates were subjected to western blot analysis using the indicated antibodies. The upper band in the pSrc blot (arrow) is the specific pSrc band. Reducing Axl expression attenuated the ability of Src to activate Akt. Figure source data can be found in Supplementary data.

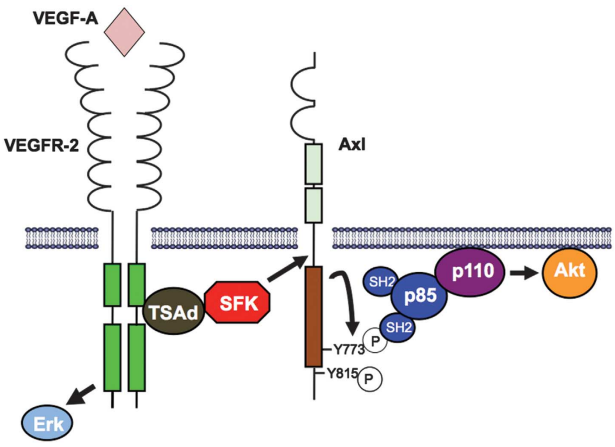

Figure 5 Model for VEGF-A-dependent activation of PI3K/Akt in endothelial cells. VEGF-A triggers a series of intracellular events that include activation of VEGFR-2 that activates SFKs in a TSAd-dependent manner. Activated SFKs engage Axl via its JM domain and thereby promote autophosphorylation at Y773 and Y815. These tyrosines reside within the optimal motifs to bind to the SH2 domains of p85 to recruit p85 and activate PI3K, which produces lipids that are essential for activation of Akt. Other VEGF-A-triggered signalling pathways (such as Erk) are independent of Axl. TSAd, T cell-specific adaptor protein; SFK, Src family kinase.

Taken together, our data indicate that activation of PI3K/Akt in response to VEGF-A proceeds intracellularly and involves the concerted action of three tyrosine kinases: VEGFR-2, SFKs and Axl (Figure 5). VEGFR-2 acts through TSAd to activate SFKs, which communicate with Axl via its JM domain to promote autophosphorylation of the two YXXM motif tyrosines, and thereby engage the PI3K/Akt pathway. Other VEGF-A-triggered signalling pathways (such as Erk and SFKs) are independent of Axl.

VEGF-A-driven migration, permeability and tube formation are dependent on Axl

The PI3K/Akt pathway is essential for several VEGF-A-induced cellular responses including cell migration, permeability and tube formation (Olsson *et al*, 2006). Our biochemical studies predict that such responses will be compromised when Axl function or expression is inhibited. Indeed, silencing Axl expression abolished VEGF-A-induced migration, but left bFGF-induced migration unchanged (Figure 6A). Similarly, VEGF-A- but not bFGF-induced migration was reduced in dominant-negative Axl mutant-expressing cells (Supplementary Figure S14). Consistent with the work of other groups identifying either SFKs or PI3K/Akt as essential contributors to VEGF-A-mediated permeability (Eliceiri *et al*, 1999; Six *et al*, 2002; Ackah *et al*, 2005; Holmes *et al*, 2007), pharmacologically inhibiting either Axl or PI3K blocked VEGF-A-dependent permeability (Figure 6B). In contrast, R428 or LY294002 did not significantly change histamine- or thrombin-dependent permeability (Figure 6B). Finally, silencing Axl expression in primary endothelial cells (HUVECs) greatly attenuated both VEGF-A-induced Akt activation (Figure 6C) and tube formation (Figure 6D; Supplementary Figure S15). Collectively, these *in-vitro* findings indicate that VEGF-A-driven cellular responses that involve PI3K/Akt are also dependent on Axl.

VEGF-A-dependent vascular permeability and corneal neovascularization are dependent on Axl

Next, we tested if Axl played a role in VEGF-A-induced vascular permeability *in vivo* by subjecting wild-type and Axl KO mice to the standard Miles assay (Miles and Miles, 1952; Six *et al*, 2002). VEGF-A or histamine was injected intradermally into WT or Axl KO mice that had received an intravenous injection of Evans blue dye. VEGF-A induced a 2.4-fold increase in Evans blue extravasation in WT mice, whereas this response was reduced to 1.2-fold in Axl KO mice (Figure 7A). There was no significant difference in histamine-induced Evans blue extravasation between WT and Axl KO mice (Figure 7A). We conclude that Axl is required for maximal VEGF-A-driven vascular permeability.

We also investigated the requirement for Axl in VEGF-A-driven angiogenesis in the standard mouse corneal

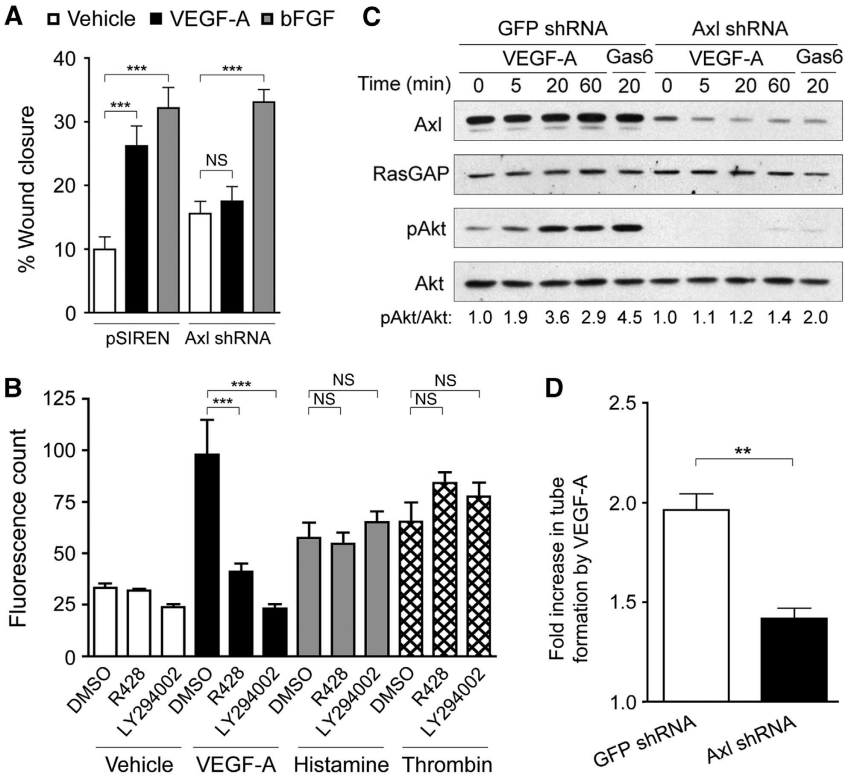

Figure 6 PI3K-mediated cellular responses in response to VEGF-A are dependent on Axl. (**A**) VEGF-A-dependent migration/wound healing is dependent on Axl. After a wound was made, PAE/KDR cells stably expressing pSIREN or Axl shRNA were treated with vehicle (white bars), 10 ng/ml VEGF-A (black bars), or 20 ng/ml bFGF (grey bars). The wound area at time 0 was normalized to 1, and '% wound closure' is the reduction of relative wound area after 18 h treatment. The data presented are mean + s.e.m. ($N = 12$). ***$P < 0.001$; 'n.s.', no significant difference. (**B**) VEGF-A-dependent *in-vitro* permeability is dependent on Axl and PI3K. HUVEC monolayers were serum starved, and pretreated with DMSO, R428 (200 nM) or LY294002 (10 μM) for 30 min, then treated with vehicle (white bars), VEGF-A (25 ng/ml; black bars), histamine (50 μM; grey bars) or thrombin (10 U/ml; cross-hatched bars) for 1 h. Permeability was determined by quantifying the fluorescence of FITC-dextran that crossed the HUVEC monolayer. The data shown are mean + s.e.m. ($N = 5$). ***$P < 0.001$; 'NS', no significant difference. (**C**) Serum-starved HUVECs stably expressing GFP or Axl shRNA were treated with VEGF-A (2.5 ng/ml) or Gas6 (100 ng/ml) for the indicated times. Cell lysates were subjected to western blot analysis using the indicated antibodies. Silencing Axl decreased both Gas6- and VEGF-A-induced Akt activation. (**D**) Fold increase in VEGF-A-stimulated tube formation compared with control. HUVECs stably expressing GFP or Axl shRNA were plated within a collagen sandwich gel, and then medium with or without 10 ng/ml VEGF-A was added. After 15 h, the tubes were photographed; representative photos are presented in Supplementary Figure S15. The data shown are mean + s.e.m. of three independent experiments. **$P < 0.01$. Silencing Axl significantly reduced VEGF-A-dependent tube formation. Figure source data can be found in Supplementary data.

micropocket assay (Rogers *et al*, 2007). Control pellets, which did not contain growth factor, failed to promote angiogenesis (Figure 7D). In WT mice, pellets containing VEGF-A induced robust corneal neovascularization, and this response was reduced by 64% in Axl KO mice (Figure 7B–D). In contrast, there was no significant difference in bFGF-induced corneal neovascularization between WT and Axl KO mice (Figure 7D). Therefore, optimal VEGF-A- but not bFGF-driven corneal neovascularization is dependent on Axl.

Discussion

Here, we report a novel mechanism by which RTKs engage the PI3K/Akt pathway (Figure 5). Upon activation with VEGF-A, VEGFR-2 acts through SFKs to promote ligand-independent autophosphorylation of Axl at YXXM motif tyrosine residues, and thereby associate with PI3K and activate Akt. These observations identify Axl as a previously unappreciated contributor to VEGF-A-dependent signalling pathways. Furthermore, we report that Axl is required for VEGF-A-dependent migration, tube formation, vascular permeability and corneal neovascularization.

Canonical adaptor proteins by which RTKs activate PI3K (such as Gab1 and insulin receptor substrates) typically do not have kinase activity. Identification of Axl, which is an RTK itself, expands our current definition of an adaptor protein. In addition to passive adaptors that need only to be phosphorylated to become functional, there also appear to be participating adaptors, which use their own kinase activity to achieve the functional state.

Identification of Axl as a required contributor to VEGF-A-driven responses provides novel insights. For instance, given that transcription of *axl* is under the control of hypoxia-inducible factor 1α (HIF-1α) and the mRNA level of Axl in endothelial cells increases in response to hypoxia (Manalo *et al*, 2005), hypoxia may coordinately upregulate the levels of VEGF-A (Forsythe *et al*, 1996), SFKs (Knock *et al*, 2008) and Axl, and thereby maximize activation of PI3K/Akt, which is likely to enforce neovascularization.

Dance *et al* (2006) reported that Gab1 plays an important role in acute (5 min) activation of PI3K/Akt in VEGF-A-stimulated PAE/KDR cells. Consequently, we were puzzled by our results that silencing Gab1 in these cells did not significantly change VEGF-A-dependent Akt activation, even

at 5 min post VEGF-A stimulation. Non-identical experimental conditions between the Dance *et al* study and our work may account for the different results.

While our studies support the emerging idea that activation of PI3K/Akt is required for VEGF-A-dependent angiogenesis, it is important to note that activation of PI3K/Akt is not sufficient to drive angiogenesis. Gas6 activates PI3K/Akt via Axl; yet, we and others observed that Gas6 did not promote tube formation (Gallicchio *et al*, 2005) (unpublished observations). Furthermore, there are no publications reporting that Gas6 is pro-angiogenic. The finding that Gas6 did not engage certain VEGF-A-dependent downstream signalling effectors, such as Erk (Figure 2A), may account for the inability of Gas6 to promote angiogenic responses.

Given the important role of Axl in VEGF-A-dependent activation of PI3K/Akt, it is a surprise that Axl KO mice are viable and fertile (Lu *et al*, 1999). Additional examples of genes whose critical function lies outside of viability and fertility include placental growth factor (PlGF), which is dispensable for embryonic angiogenesis, yet its deficiency interferes with pathological angiogenesis (Carmeliet *et al*, 2001). We noticed that in the lung lysates and lung endothelial cells prepared from Axl KO mice, basal Akt activation was markedly increased (unpublished observations). Thus, endothelial cells in Axl KO mice might elevate overall PI3K/Akt activation to reduce their dependence on VEGF-A for PI3K/Akt activation. It is also possible that Axl is not the only mediator of VEGF-A-dependent activation of PI3K/Akt, or that the function and/or expression of other adaptor proteins (such as Gab1 and/or Shb) are elevated in the absence of Axl.

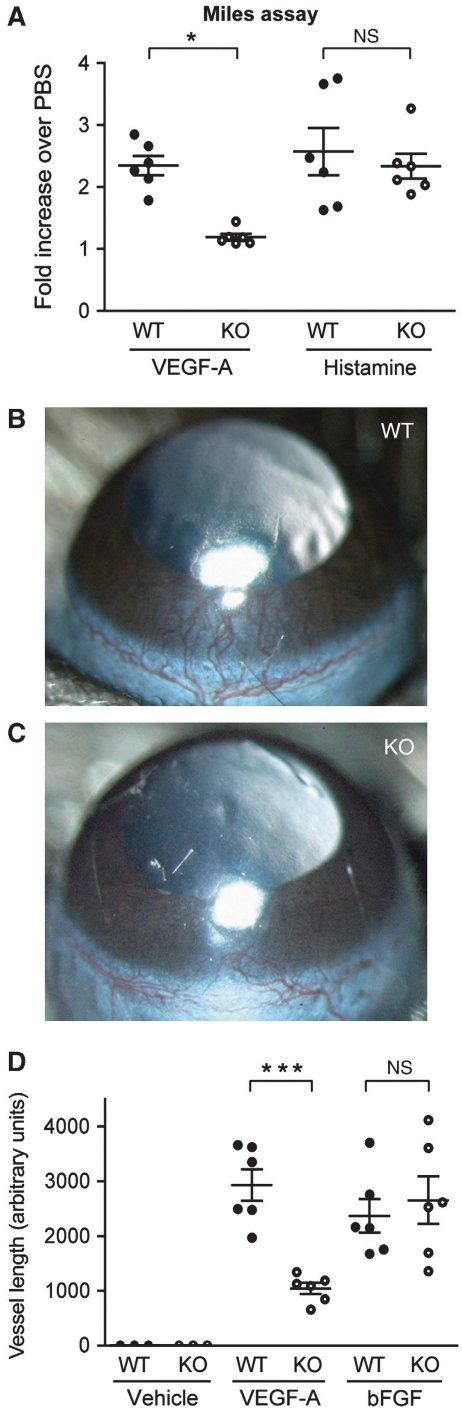

Materials and methods

Animals

Axl KO mice were created and characterized by Deltagen, Inc. (San Carlos, CA), and distributed by The Jackson Laboratory (Bar Harbor, ME; Stock Number: 005777). In these KO mice, Axl expression is disrupted by a bacterial *lacZ* gene. The KO mice had been backcrossed at least eight generations to C57BL/6J mice. The age of the Axl KO mice and background matched wild-type mice that were used for the Miles assay and corneal micropocket angiogenesis assay was 8–12 weeks. All animal use was approved by the Schepens Animal Care and Use Committee and conducted in accordance with the guidelines of the Association for Research in Vision and Ophthalmology (ARVO) Statement for the Use of Animals.

Antibodies and reagents

Recombinant human VEGF-A_{165} and bFGF were generously provided by the National Cancer Institute's Biological Resources Branch (Rockville, MD). The Axl inhibitor R428 was kindly provided by Dr Sacha J Holland at the Rigel Pharmaceuticals, Inc. (South San Francisco, CA). Gas6, AxlFc, antibodies against TSAd and the extracellular domain of Axl (used for AxlJdn, AxlTdn and AxlJdn3F), and horseradish peroxidase (HRP)-conjugated donkey anti-sheep IgG secondary antibody were purchased from R&D Systems (Minneapolis, MN). LY294002 and antibodies against phospho-Axl (Y702), Axl (used to detect endogenous Axl),

Figure 7 VEGF-A-driven vascular permeability and corneal neovascularization are dependent on Axl. (**A**) Miles assay showing VEGF-A-dependent vascular permeability was greatly attenuated in Axl KO mice. The right dorsal side of mice that had been intravenously injected with Evans blue dye received four intradermal injections of VEGF-A (100 ng in 50 μl PBS) or histamine (2.5 nmol in 50 μl PBS). The left dorsal side of mice received four intradermal injections of PBS (50 μl). The Evans blue extravasation induced by VEGF-A, histamine or PBS was measured spectrophotometrically at 630 nm. The data presented are the ratio of VEGF-A- or histamine-induced Evans blue extravasation to PBS-induced extravasation from the same animal. The horizontal bars indicate the mean ± s.e.m. ($N=6$). *$P<0.05$; 'NS', no significant difference. (**B**, **C**) Representative images of corneal neovascularization induced by VEGF-A in WT (**B**) and Axl KO (**C**) mice. Pellets containing vehicle, VEGF-A (160 ng) or bFGF (80 ng) were implanted into the corneas. Corneal neovascularization was imaged 7 days after pellet implantation with a slit lamp camera. (**D**) Quantification of total length of blood vessels induced by vehicle ($N=3$), VEGF-A ($N=6$) or bFGF pellet ($N=6$). The horizontal bars indicate mean ± s.e.m. ***$P<0.001$; 'NS', no significant difference.

phospho-Akt (S473), Akt, phospho-Erk, Erk, phospho-Src (Y416), Src, phospho-VEGFR-2 (Y1175), Gab1 were purchased from Cell Signalling Technology (Beverly, MA). Mouse monoclonal antibodies 4G10 and anti-p85 were purchased from Millipore (Temecula, CA). The other anti-phosphotyrosine antibody PY20 was purchased from BD Transduction Laboratories (San Diego, CA). Rabbit polyclonal anti-RasGAP and anti-VEGFR-2 antibodies were produced in the Kazlauskas laboratory as previously described (Klinghoffer *et al*, 1996; Rahimi and Kazlauskas, 1999). HRP-conjugated goat anti-rabbit IgG, goat anti-mouse IgG and goat anti-rat IgG secondary antibodies were purchased from Santa Cruz Biotechnology (Santa Cruz, CA). Enhanced chemiluminescent substrate for detection of HRP was purchased from Pierce Protein Research Products (Rockford, IL). SU6656 was purchased from Calbiochem (La Jolla, CA). All other chemicals and reagents were obtained from Sigma (St Louis, MO) unless otherwise indicated.

Cell culture

PAE/KDR cells (Waltenberger *et al*, 1994) were cultured in a 1:1 mixture of low-glucose Dulbecco's modified Eagle's medium (DMEM; Gibco, Grand Island, NY) and Ham's F-12 Nutrient Mixture (Gibco), which was supplemented with 10% fetal bovine serum (FBS; Lonza, Walkersville, MD), and 100 U/ml penicillin G and 100 μg/ml streptomycin (Gemini BioProducts, West Sacramento, CA). HUVECs (Lonza) and HRMECs (Cell Systems, Kirkland, WA) were plated on tissue culture dishes that had been precoated with 0.2% gelatin, and cultured in Medium 199 (Sigma) supplemented with 20% bovine calf serum (BCS; HyClone, Logan, UT), 100 μg/ml heparin, 12 μg/ml bovine brain extract (BBE; Hammond Cell Tech, Windsor, CA), and penicillin G and streptomycin. 293GPG cells (Ory *et al*, 1996) were cultured in high-glucose DMEM supplemented with 10% FBS, 1 μg/ml tetracycline, 2 μg/ml puromycin, 0.3 mg/ml G418, 16.7 mM HEPES (Lonza), and penicillin G and streptomycin. The medium used to collect retroviral supernatant from 293GPG cells was high-glucose DMEM supplemented with 10% FBS, 16.7 mM HEPES, and penicillin G and streptomycin. 293T cells were cultured in high-glucose DMEM supplemented with 10% FBS, and 10 U/ml penicillin G and 10 μg/ml streptomycin. The medium used to harvest lentiviral supernatant from 293T cells was high-glucose DMEM supplemented with 30% FBS, and 100 U/ml penicillin G and 100 μg/ml streptomycin. All cells were cultured at 37°C in a humidified 5% CO_2 atmosphere.

Retroviral shRNA knockdown of Axl and Gab1 in PAE/KDR cells

To suppress the expression of Gab1 and Axl in PAE/KDR cells, two shRNAs against Gab1 and one shRNA against Axl (sequences are listed in Supplementary Table S1) were synthesized as single-stranded DNA oligos by the DNA core facility of Massachusetts General Hospital (MGH), annealed into double-stranded oligos, and cloned into the *Bam*HI-*Eco*RI sites of the retroviral vector RNAi-Ready pSIREN-RetroQ (Clontech, Mountain View, CA). The plasmids were transfected into 293GPG cells using Lipofectamine Plus (Invitrogen) to obtain retroviral supernatants, which were used to infect PAE/KDR cells. The successfully infected cells were selected for the ability to proliferate in medium containing puromycin (1 μg/ml).

Lentiviral shRNA knockdown of Axl and TSAd in HUVECs

The hairpin-pLKO.1 retroviral vector containing shRNAs for GFP, Axl or TSAd (sequences are listed in Supplementary Table S1), the packaging plasmid (pCMV-ΔR8.91), the envelope plasmid (VSV-G/pMD2.G) and 293T packaging cells were obtained from iLab Solutions (Dana-Farber Cancer Institute, Harvard Medical School, Boston, MA).

To prepare shRNA lentivirus, a mixture of packaging plasmid (900 ng), envelope plasmid (100 ng), hairpin-pLKO.1 vector (1 μg), and Mirus TransIT-LT1 reagent (Mirus Bio, Madison, WI) was incubated at room temperature for 30 min and transferred to the 293T packaging cells (in low-antibiotic growth medium). At 18 h post transfection, the medium was replaced with DMEM containing 30% FBS, and retroviral supernatant was harvested 40 and 64 h post transfection. The retroviral supernatant was pooled and used to infect HUVECs. The successfully infected cells were selected for the ability to proliferate in medium containing puromycin (1 μg/ml).

Stable expression of Axlwt, Axlkd and F73/15 mutants in Axl-deficient PAE/KDR cells

Mouse Axl cDNA (clone ID: 6418252) was obtained from Open Biosystems (Huntsville, AL), and subcloned into the *Not*I-*Bam*HI sites of the retroviral vector pLXSHD[2] vector. Point mutations of Lys561 to Arg (Axlkd), or Tyr773 and Try815 to Phe (F73/15) were introduced into the pLXSHD[2]-Axlwt plasmid using the QuikChange XL site-directed mutagenesis kit following manufacturer's instructions (Stratagene, La Jolla, CA). The primer sequences used for site mutations are listed in Supplementary Table S1. The mutations were confirmed by DNA sequencing at the MGH DNA core facility. The plasmids were transfected into 293GPG cells using Lipofectamine Plus to obtain retroviral supernatant, which was used to infect Axl-deficient PAE/KDR cells. The successfully infected cells were selected for their ability to proliferate in histidine-free medium supplemented with 1 mM histidinol.

Stable expression of AxlJdn, AxlTdn and AxlJdn3F in PAE/KDR cells

The 1–529 amino-acid fragment of Axl (AxlJdn) and the 1–469 amino-acid fragment of Axl (AxlTdn) were each cloned into the *Hin*dIII-*Not*I sites of pLPCX. Point mutations of Tyr475, Tyr492 and Try498 to Phe (AxlJdn3F) were introduced into the pLPCX-AxlJdn plasmid using the QuikChange XL site-directed mutagenesis kit (Stratagene). The primer sequences used for site mutations are listed in Supplementary Table S1. The mutant sequences were confirmed by DNA sequencing at the MGH DNA core facility. The plasmids were transfected into 293GPG cells using Lipofectamine Plus to obtain retroviral supernatant, which was used to infect PAE/KDR cells. The successfully infected cells were selected for their ability to proliferate in the presence of 1 μg/ml of puromycin.

R388A and D386N Src mutants

The Src mutants SrcR388A/Y527F (R388A) and SrcD386N/Y527F (D386N) were previously described (Qiao *et al*, 2006; Im and Kazlauskas, 2007). The cDNAs were subcloned into the *Eco*RI-*Bam*HI sites of the retroviral vector pLXSHD[2] vector. The resulting plasmids were transfected into 293GPG cells using Lipofectamine Plus to obtain retroviral supernatant, which was used to infect PAE/KDR cells. The successfully infected cells were selected for their ability to proliferate in histidine-free medium supplemented with 1 mM histidinol.

Western blot analysis

Cells plated in 24-well plates were grown to 80% confluence, serum starved for 24 h and then treated with reagents specified in each figure. The dose of VEGF-A that we routinely used in biochemical experiments was 2.5 ng/ml VEGF-A. The responses observed at this dose were comparable to those seen with 50 ng/ml VEGF-A (Supplementary Figure S4). The cells were washed twice with ice-cold PBS, and then lysed in sample buffer (100 mM Tris–HCl (pH 6.8), 5 mM EDTA, 100 mM dithiothreitol (DTT), 10% glycerol, 2% sodium dodecyl sulphate (SDS), 0.5% bromophenol blue) supplemented with 2 mM sodium orthovanadate, 1 mM phenylmethylsulphonyl fluoride (PMSF), and 100 mM 2-mercaptoethanol. The total cell lysates were subjected to SDS–PAGE and then immunoblotted with desired antibodies. The resultant data were quantified densitometrically with Quantity One software (Bio-Rad Laboratories, Hercules, CA). To reprobe a blot, the membrane was first stripped by incubating for 30 min at 60°C in stripping buffer (62.5 mM Tris–HCl (pH 6.8), 2% SDS, 100 mM 2-mercaptoethanol), and then reprobed with desired antibodies. The blotting data that are shown are representative of at least three independent experiments.

GST pull-down assay

The N-terminal SH2 domain (residues 334–430) of human p85α (accession number: AAH94795) was cloned into the *Bam*HI-*Eco*RI sites of the GST expression vector pGEX-2T (GE Healthcare, Piscataway, NJ). The nucleotide sequences were confirmed by sequencing at the MGH DNA core facility. Expression of GST or GST-p85SH2 fusion protein was induced with 0.1 mM isopropylthio-galactopyranoside (IPTG) overnight at 25°C, and purified using glutathione-agarose 4B beads according to the manufacturer instructions (GE Healthcare).

Cells plated on 10 cm culture dishes were grown to 70–80% confluence, serum starved, pretreated with 100 μM sodium ortho-

vanadate for 1 h, and then left resting, or treated with VEGF-A (2.5 ng/ml) for 5, 20 or 60 min. The cells were washed three times with ice-cold PBS, lysed in extraction buffer (10 mM Tris–HCl (pH 7.4), 5 mM EDTA, 50 mM NaCl, 50 mM NaF, 1% Triton X-100, 20 μg/ml aprotinin, 2 mM sodium orthovanadate, 1 mM PMSF). For GST pull-down assay, 4 μg of GST or GST-p85SH2 fusion protein bound to glutathione-agarose beads was incubated with 100 μg of clarified cell lysate at 4°C for 1 h on a rocking platform. After incubation, the resin was washed twice with 1 ml of RIPA buffer (150 mM NaCl, 10 mM Na_2HPO_4, 10 mM NaH_2PO_4, 2 mM EDTA, 1% sodium deoxycholate, 1% NP-40, 0.1% SDS, 20 μg/ml aprotinin, 50 mM NaF, 14 mM 2-mercaptoethanol, 2 mM sodium orthovanadate, 1 mM PMSF), followed by one wash with 1 ml of extraction buffer. Bound proteins were eluted by boiling in sample buffer, separated by SDS–PAGE and immunoblotted with indicated antibodies.

Immunoprecipitation

Precleared cell lysate (500 μg) collected as in 'GST Pull-down Assay' was combined with anti-Axl antibody as the precipitating antibody and the sample was incubated overnight at 4°C on a rocking platform. Protein A-Agarose (Santa Cruz Biotechnology) was then added and incubated at 4°C for another 1 h. Beads were then sedimented, washed three times with extraction buffer. Bound proteins were eluted by boiling in sample buffer, separated by SDS–PAGE and immunoblotted with indicated antibodies.

Preparation of MHECs

MHECs were isolated from 8- to 12-week-old wild-type and Axl KO mice as outlined in a previously described protocol (Lim and Luscinskas, 2006). Cells at passage 3 were used in the current study.

Wound healing assay

The wound healing assay was performed as previously described (Rodriguez *et al*, 2005) with some modifications. Once cells reached 80% confluence in 24-well plates they were starved for 24 h. A wound was created by scraping the cell monolayer with a sterile pipette tip. The cells were washed twice to remove detached cells, and then 1 ml of serum-free medium containing vehicle, VEGF-A (10 ng/ml) or bFGF (20 ng/ml) was added. The wound was photographed at time 0 and 18 h post wounding with a SPOT camera attached to a Nikon Eclipse TE2000-S inverted microscope (Nikon, Melville, NY). Quantification was done by measuring the number of pixels in the wound area using Adobe Photoshop (Adobe Systems, San Jose, CA).

In-vitro permeability assay

The permeability assay was performed according to the product manual (*In vitro* Vascular Permeability Assay from Millipore: ECM642). HUVEC at passage 5 was seeded at 80 000 cells per insert and cultured for 72 h in HUVEC culture medium. Cells were serum starved for 3 h, pretreated with DMSO, R428 (200 nM) or LY294002 (10 μM) for 30 min, then treated with vehicle, VEGF-A (25 ng/ml), histamine (50 μM) or thrombin (10 U/ml) for 1 h. FITC-dextran was added to the semipermeable insert and incubated at room temperature for 30 min. The extent of permeability was determined by measuring the fluorescence (excitation/emission wavelength of 485 nm/530 nm) in the medium beneath the cell-coated inserts.

Tube formation assay

A collagen gel mixture consisting of 80% (by volume) collagen (Devro Pty, Sydney, Australia), 1.6 mg/ml NaOH, 2 mg/ml $NaHCO_3$, 20 mM HEPES (Lonza), 0.5 μg/ml fibronectin, 0.5 μg/ml laminin and 10.4 mg/ml RPMI powder (GIBCO) was prepared. For the lower gel layer, 200 μl of the gel mixture was added to each well of the 48-well plates and incubated at 37°C for 1 h. After polymerization, 3×10^4 HUVECs stably expressing GFP shRNA or Axl shRNA were seeded in each well and incubated with EBM (Lonza) containing 5% horse serum (Sigma) and 12 μg/ml BBE for 24 h at 37°C. The medium was removed and 80 μl of the gel mixture was added to each well. The plates were incubated at 37°C for 1 h to polymerize the upper gel layer. EBM with or without 10 ng/ml VEGF-A was then added to each well. Tubes were photographed 15 h after treatment with a SPOT camera attached to a Nikon Eclipse TE2000-S inverted Microscope. After calibration with a stage micrometer, the total tube length within a field was quantified using the Image J software (NIH, Bethesda, MD).

Miles assay

Miles assay was performed as previously described (Eliceiri *et al*, 1999) with slight modifications. Briefly, under anaesthesia, mice were intravenously injected with 100 μl of 0.25% Evans blue. VEGF-A_{165} (100 ng in 50 μl PBS) or histamine (2.5 nmol in 50 μl PBS) was injected intradermally into the skin on the right dorsal side of the preshaved mouse, while 50 μl of PBS was injected intradermally on the left dorsal side. After 30 min, mice were euthanized and epidermis surrounding the injection site (~5 mm in diameter) was surgically removed. The evans blue was eluted from the surgical specimens by incubating in 500 μl of formamide for 24 h at 55°C. The amount of evans blue was measured spectrophotometrically at 630 nm using a standard curve of Evans blue in formamide.

Corneal micropocket angiogenesis assay

Corneal micropocket angiogenesis assay was performed as previously described (Rogers *et al*, 2007; Im *et al*, 2010). Briefly, corneal micropockets were created with a modified von Graefe knife. Hydron pellets containing 160 ng of VEGF-A_{165}, 80 ng of bFGF or hydron pellets without growth factor were implanted into the corneal pockets. Corneal neovascularization was photographed with a slit lamp biomicroscope (model FS-2; Nikon) on day 7 after pellet implantation. The blood vessels were quantified using the Image J software.

Statistical analysis

Data are presented as the mean ± s.e.m. Comparisons between two groups were performed using Student's *t*-test. Comparisons for multiple groups were performed using one-way ANOVA followed by Tukey's HSD *post hoc* test.

Supplementary data

Supplementary data are available at *The EMBO Journal* Online (http://www.embojournal.org).

Acknowledgements

We would like to thank Drs Lena Claesson-Welsh and Xiujuan Li (Uppsala University, Sweden) for advice on TSAd experiments. We appreciate the suggestions and input from the following members of the Kazlauskas laboratory: Sarah Melissa P Jacob, Hetian Lei, Steven Pennock, Kevin Conway, Ruta Motiejunaite, Jorge Aranda, Eun Young Park and Magdalena Staniszewska. This work was supported by Juvenile Diabetes Research Foundation (JDRF) grant 12008905 (to AK), NIH grant EY016385 (to AK), JDRF postdoctoral fellowship 32009560 (to GXR) and JDRF advanced postdoctoral fellowship 102011367 (to GXR).

Author contributions: AK and GXR are responsible for all aspects of this paper except performing experiments, which was done exclusively by GXR.

Conflict of interest

The authors declare that they have no conflict of interest.

References

Ackah E, Yu J, Zoellner S, Iwakiri Y, Skurk C, Shibata R, Ouchi N, Easton RM, Galasso G, Birnbaum MJ, Walsh K, Sessa WC (2005) Akt1/protein kinase Balpha is critical for ischemic and VEGF-mediated angiogenesis. *J Clin Invest* **115:** 2119–2127

Braunger J, Schleithoff L, Schulz AS, Kessler H, Lammers R, Ullrich A, Bartram CR, Janssen JW (1997) Intracellular signaling of the Ufo/Axl receptor tyrosine kinase is mediated mainly by a multi-substrate docking-site. *Oncogene* **14:** 2619–2631

Brown DM, Kaiser PK, Michels M, Soubrane G, Heier JS, Kim RY, Sy JP, Schneider S (2006) Ranibizumab versus verteporfin for neovascular age-related macular degeneration. *N Engl J Med* **355:** 1432–1444

Carmeliet P, Ferreira V, Breier G, Pollefeyt S, Kieckens L, Gertsenstein M, Fahrig M, Vandenhoeck A, Harpal K, Eberhardt C, Declercq C, Pawling J, Moons L, Collen D, Risau W, Nagy A (1996) Abnormal blood vessel development and lethality in embryos lacking a single VEGF allele. *Nature* **380:** 435–439

Carmeliet P, Moons L, Luttun A, Vincenti V, Compernolle V, De Mol M, Wu Y, Bono F, Devy L, Beck H, Scholz D, Acker T, DiPalma T, Dewerchin M, Noel A, Stalmans I, Barra A, Blacher S, Vandendriessche T, Ponten A *et al* (2001) Synergism between vascular endothelial growth factor and placental growth factor contributes to angiogenesis and plasma extravasation in pathological conditions. *Nat Med* **7:** 575–583

Cross MJ, Dixelius J, Matsumoto T, Claesson-Welsh L (2003) VEGF-receptor signal transduction. *Trends Biochem Sci* **28:** 488–494

Cully M, You H, Levine AJ, Mak TW (2006) Beyond PTEN mutations: the PI3K pathway as an integrator of multiple inputs during tumorigenesis. *Nat Rev Cancer* **6:** 184–192

Dance M, Montagner A, Yart A, Masri B, Audigier Y, Perret B, Salles JP, Raynal P (2006) The adaptor protein Gab1 couples the stimulation of vascular endothelial growth factor receptor-2 to the activation of phosphoinositide 3-kinase. *J Biol Chem* **281:** 23285–23295

Eliceiri BP, Paul R, Schwartzberg PL, Hood JD, Leng J, Cheresh DA (1999) Selective requirement for Src kinases during VEGF-induced angiogenesis and vascular permeability. *Mol Cell* **4:** 915–924

Ferrara N (2009) VEGF-A: a critical regulator of blood vessel growth. *Eur Cytokine Netw* **20:** 158–163

Ferrara N, Carver-Moore K, Chen H, Dowd M, Lu L, O'Shea KS, Powell-Braxton L, Hillan KJ, Moore MW (1996) Heterozygous embryonic lethality induced by targeted inactivation of the VEGF gene. *Nature* **380:** 439–442

Ferrara N, Gerber HP, LeCouter J (2003) The biology of VEGF and its receptors. *Nat Med* **9:** 669–676

Forsythe JA, Jiang BH, Iyer NV, Agani F, Leung SW, Koos RD, Semenza GL (1996) Activation of vascular endothelial growth factor gene transcription by hypoxia-inducible factor 1. *Mol Cell Biol* **16:** 4604–4613

Gallicchio M, Mitola S, Valdembri D, Fantozzi R, Varnum B, Avanzi GC, Bussolino F (2005) Inhibition of vascular endothelial growth factor receptor 2-mediated endothelial cell activation by Axl tyrosine kinase receptor. *Blood* **105:** 1970–1976

Holland SJ, Pan A, Franci C, Hu Y, Chang B, Li W, Duan M, Torneros A, Yu J, Heckrodt TJ, Zhang J, Ding P, Apatira A, Chua J, Brandt R, Pine P, Goff D, Singh R, Payan DG, Hitoshi Y (2010) R428, a selective small molecule inhibitor of Axl kinase, blocks tumor spread and prolongs survival in models of metastatic breast cancer. *Cancer Res* **70:** 1544–1554

Holland SJ, Powell MJ, Franci C, Chan EW, Friera AM, Atchison RE, McLaughlin J, Swift SE, Pali ES, Yam G, Wong S, Lasaga J, Shen MR, Yu S, Xu W, Hitoshi Y, Bogenberger J, Nor JE, Payan DG, Lorens JB (2005) Multiple roles for the receptor tyrosine kinase axl in tumor formation. *Cancer Res* **65:** 9294–9303

Holmes K, Roberts OL, Thomas AM, Cross MJ (2007) Vascular endothelial growth factor receptor-2: structure, function, intracellular signalling and therapeutic inhibition. *Cell Signal* **19:** 2003–2012

Im E, Kazlauskas A (2006) Regulating angiogenesis at the level of PtdIns-4,5-P2. *EMBO J* **25:** 2075–2082

Im E, Kazlauskas A (2007) Src family kinases promote vessel stability by antagonizing the Rho/ROCK pathway. *J Biol Chem* **282:** 29122–29129

Im E, Motiejunaite R, Aranda J, Park EY, Federico L, Kim TI, Clair T, Stracke ML, Smyth S, Kazlauskas A (2010) Phospholipase Cgamma activation drives increased production of autotaxin in endothelial cells and lysophosphatidic acid-dependent regression. *Mol Cell Biol* **30:** 2401–2410

Kazlauskas A, Cooper JA (1989) Autophosphorylation of the PDGF receptor in the kinase insert region regulates interactions with cell proteins. *Cell* **58:** 1121–1133

Kerbel RS (2008) Tumor angiogenesis. *N Engl J Med* **358:** 2039–2049

Klinghoffer RA, Duckworth B, Valius M, Cantley L, Kazlauskas A (1996) Platelet-derived growth factor-dependent activation of phosphatidylinositol 3-kinase is regulated by receptor binding of SH2-domain-containing proteins which influence Ras activity. *Mol Cell Biol* **16:** 5905–5914

Knock GA, Snetkov VA, Shaifta Y, Drndarski S, Ward JP, Aaronson PI (2008) Role of src-family kinases in hypoxic vasoconstriction of rat pulmonary artery. *Cardiovasc Res* **80:** 453–462

Kypta RM, Goldberg Y, Ulug ET, Courtneidge SA (1990) Association between the PDGF receptor and members of the src family of tyrosine kinases. *Cell* **62:** 481–492

Laramee M, Chabot C, Cloutier M, Stenne R, Holgado-Madruga M, Wong AJ, Royal I (2007) The scaffolding adapter Gab1 mediates vascular endothelial growth factor signaling and is required for endothelial cell migration and capillary formation. *J Biol Chem* **282:** 7758–7769

Li Y, Ye X, Tan C, Hongo JA, Zha J, Liu J, Kallop D, Ludlam MJ, Pei L (2009) Axl as a potential therapeutic target in cancer: role of Axl in tumor growth, metastasis and angiogenesis. *Oncogene* **28:** 3442–3455

Lim YC, Luscinskas FW (2006) Isolation and culture of murine heart and lung endothelial cells for *in vitro* model systems. *Methods Mol Biol* **341:** 141–154

Lu Q, Gore M, Zhang Q, Camenisch T, Boast S, Casagranda F, Lai C, Skinner MK, Klein R, Matsushima GK, Earp HS, Goff SP, Lemke G (1999) Tyro-3 family receptors are essential regulators of mammalian spermatogenesis. *Nature* **398:** 723–728

Manalo DJ, Rowan A, Lavoie T, Natarajan L, Kelly BD, Ye SQ, Garcia JG, Semenza GL (2005) Transcriptional regulation of vascular endothelial cell responses to hypoxia by HIF-1. *Blood* **105:** 659–669

Matsumoto T, Bohman S, Dixelius J, Berge T, Dimberg A, Magnusson P, Wang L, Wikner C, Qi JH, Wernstedt C, Wu J, Bruheim S, Mugishima H, Mukhopadhyay D, Spurkland A, Claesson-Welsh L (2005) VEGF receptor-2 Y951 signaling and a role for the adapter molecule TSAd in tumor angiogenesis. *EMBO J* **24:** 2342–2353

Matsumoto T, Claesson-Welsh L (2001) VEGF receptor signal transduction. *Sci STKE* **2001:** re21

McCloskey P, Fridell YW, Attar E, Villa J, Jin Y, Varnum B, Liu ET (1997) GAS6 mediates adhesion of cells expressing the receptor tyrosine kinase Axl. *J Biol Chem* **272:** 23285–23291

Melaragno MG, Fridell YW, Berk BC (1999) The Gas6/Axl system: a novel regulator of vascular cell function. *Trends Cardiovasc Med* **9:** 250–253

Miles AA, Miles EM (1952) Vascular reactions to histamine, histamine-liberator and leukotaxine in the skin of guinea-pigs. *J Physiol* **118:** 228–257

Nishijima K, Ng YS, Zhong L, Bradley J, Schubert W, Jo N, Akita J, Samuelsson SJ, Robinson GS, Adamis AP, Shima DT (2007) Vascular endothelial growth factor-A is a survival factor for retinal neurons and a critical neuroprotectant during the adaptive response to ischemic injury. *Am J Pathol* **171:** 53–67

Olsson AK, Dimberg A, Kreuger J, Claesson-Welsh L (2006) VEGF receptor signalling - in control of vascular function. *Nat Rev Mol Cell Biol* **7:** 359–371

Ory DS, Neugeboren BA, Mulligan RC (1996) A stable human-derived packaging cell line for production of high titer retrovirus/vesicular stomatitis virus G pseudotypes. *Proc Natl Acad Sci USA* **93:** 11400–11406

Pandya NM, Dhalla NS, Santani DD (2006) Angiogenesis—a new target for future therapy. *Vascul Pharmacol* **44:** 265–274

Phung TL, Ziv K, Dabydeen D, Eyiah-Mensah G, Riveros M, Perruzzi C, Sun J, Monahan-Earley RA, Shiojima I, Nagy JA, Lin MI, Walsh K, Dvorak AM, Briscoe DM, Neeman M, Sessa WC, Dvorak HF, Benjamin LE (2006) Pathological angiogenesis is induced by sustained Akt signaling and inhibited by rapamycin. *Cancer Cell* **10:** 159–170

Qiao Y, Molina H, Pandey A, Zhang J, Cole PA (2006) Chemical rescue of a mutant enzyme in living cells. *Science* **311:** 1293–1297

Rahimi N (2006) VEGFR-1 and VEGFR-2: two non-identical twins with a unique physiognomy. *Front Biosci* **11:** 818–829

Rahimi N, Kazlauskas A (1999) A role for cadherin-5 in regulation of vascular endothelial growth factor receptor 2 activity in endothelial cells. *Mol Biol Cell* **10:** 3401–3407

Rodriguez LG, Wu X, Guan JL (2005) Wound-healing assay. *Methods Mol Biol* **294:** 23–29

Rogers MS, Birsner AE, D'Amato RJ (2007) The mouse cornea micropocket angiogenesis assay. *Nat Protoc* **2:** 2545–2550

Rohde CM, Schrum J, Lee AW (2004) A juxtamembrane tyrosine in the colony stimulating factor-1 receptor regulates ligand-induced Src association, receptor kinase function, and down-regulation. *J Biol Chem* **279:** 43448–43461

Rosenfeld PJ, Brown DM, Heier JS, Boyer DS, Kaiser PK, Chung CY, Kim RY (2006) Ranibizumab for neovascular age-related macular degeneration. *N Engl J Med* **355:** 1419–1431

Rothlin CV, Ghosh S, Zuniga EI, Oldstone MB, Lemke G (2007) TAM receptors are pleiotropic inhibitors of the innate immune response. *Cell* **131:** 1124–1136

Six I, Kureishi Y, Luo Z, Walsh K (2002) Akt signaling mediates VEGF/VPF vascular permeability *in vivo*. *FEBS Lett* **532:** 67–69

Songyang Z, Carraway KLI, Eck MJ, Harrison SC, Feldman RA, Mohammadi M, Schlessinger J, Hubbard SR, Smith DP, Eng C, Lorenzo MJ, Ponder BAJ, Mayer BJ, Cantley LC (1995) Catalytic specificity of protein-tyrosine kinases is critical for selective signalling. *Nature* **373:** 536–539

Varnum BC, Young C, Elliott G, Garcia A, Bartley TD, Fridell YW, Hunt RW, Trail G, Clogston C, Toso RJ, Yanagihara D, Bennett L, Sylber M, Merewether LA, Tseng A, Escobar E, Liu ET, Yamane HK (1995) Axl receptor tyrosine kinase stimulated by the vitamin K-dependent protein encoded by growth-arrest-specific gene 6. *Nature* **373:** 623–626

Waltenberger J, Claesson-Welsh L, Siegbahn A, Shibuya M, Heldin CH (1994) Different signal transduction properties of KDR and Flt1, two receptors for vascular endothelial growth factor. *J Biol Chem* **269:** 26988–26995

Whitehead JP, Clark SF, Urso B, James DE (2000) Signalling through the insulin receptor. *Curr Opin Cell Biol* **12:** 222–228

Wybenga-Groot LE, Baskin B, Ong SH, Tong J, Pawson T, Sicheri F (2001) Structural basis for autoinhibition of the Ephb2 receptor tyrosine kinase by the unphosphorylated juxtamembrane region. *Cell* **106:** 745–757